Eur. Phys. J. B **56**, 323–333 (2007)
DOI: 10.1140/epjb/e2007-00127-2

THE EUROPEAN PHYSICAL JOURNAL B

# Photogalvanic current in artificial asymmetric nanostructures

A.D. Chepelianskii[1], M.V. Entin[2], L.I. Magarill[2], and D.L. Shepelyansky[3,a]

[1] École Normale Supérieure, 45 rue d'Ulm, 75231 Paris Cedex 05, France
[2] Institute of Semiconductor Physics, Siberian Division of Russian Academy of Sciences, Novosibirsk, 630090, Russia
[3] Laboratoire de Physique Théorique, UMR 5152 (CNRS), Univ. P. Sabatier, 31062 Toulouse Cedex 4, France

Received 7 January 2007 / Received in final form 12 April 2007
Published online 11 May 2007 – 

**Abstract.** We develop a theoretic description of the photogalvanic current induced by a high frequency radiation in asymmetric nanostructures and show that it describes well the results of numerical simulations. Our studies allow to understand the origin of the electronic ratchet transport in such systems and show that they can be used for creation of new types of detectors operating at room temperature in a terahertz radiation range.

**PACS.** 72.40.+w Photoconduction and photovoltaic effects – 73.63.-b Electronic transport in nanoscale materials and structures – 05.45.Ac Low-dimensional chaos

## 1 Introduction

Since the experiments of Glass et al. performed in 1974 [1] and the theoretical explanations developed in 1976 [2,3] it is known that an asymmetry of crystal at a microscopic scale can lead to emergence of macroscopic stationary directed current when the crystal is irradiated by an external light source. The appearance of directed current induced by zero-mean force of radiation in absence of any external static voltage has been named the photogalvanic effect. This unusual phenomenon based on interplay of space asymmetry, relaxation and external driving had been mainly discussed for interaction of light with crystals [4,5]. However, this effect has a rather generic physical origin and the interest to it has been significantly renewed recently when it became clear that it may play an important role for transport in bio-systems where it is difficult to create static forces in space and where directed transport may be more easily generated by some oscillating parameters in presence of asymmetry at a molecular level (see e.g. a review [6]). In this community the phenomenon became known as ratchet, following an example of pawl and ratchet described by Feynman and showing that a directed transport in asymmetric systems at a thermal equilibrium is forbidden by the second law of thermodynamics [7].

The appearance of the photogalvanic or ratchet effect in various systems is described in the reviews [8,9]. The effect has been observed with vortices in Josephson junction arrays [10–12], cold atoms [13], macroporous silicon membranes [14], microfluidic channels [15] and other systems. The great variety of systems clearly confirms a generic nature of the phenomenon.

In parallel to these ratchet studies, a technological progress made possible to produce artificial superlattices in semiconductors with two-dimensional electron gas (2DES). The experimental studies of superlattices of antidots in a form of disks demonstrated an important contribution of periodic orbits in the transport properties of 2DES [16,17]. It is important to note that the interest to particle dynamics on a lattice of rigid disks goes back to the days of Galton who in far 1889 showed the appearance of statistical laws in such systems [18]. A rigorous mathematical description of chaos on the Galton board that leads to statistical laws has been given by Sinai [19]. The links between the chaotic dynamics, periodic orbits and experimental results for 2DES transport properties in antidot superlattices have been established in theoretical studies [20]. The interest to effects of microwave radiation on 2DES transport appeared at a relatively early stage, however, during a relatively long time only the case of antidots with a disk shape has been considered (see e.g. [21,22]). Due to symmetry reasons the photogalvanic effect is absent in such a case.

The experimental studies of 2DES transport in asymmetric structures in presence of *ac*-driving have been started in [23–25]. They demonstrated the principal existence of photogalvanic transport but no detailed analysis had been done for 2D structures. The quasi-1D case [24] has been analyzed in more detail but the ratchet transport in this case is rather slow due to very slow *ac*-driving. Thus, the ratchet transport in this case was linked to quantum tunneling effects (see [24] and discussions in [9]). On the contrary the experiments in 2D structures [23,25]

[a] http://www.quantware.ups-tlse.fr/dima/

have been performed at rather high frequencies (50 GHz and more) showing that high frequency control of ratchet transport is possible in principle. Moreover, the experiment [25] demonstrated that the photogalvanic current exists at room temperature. Unfortunately, there was no further development of this interesting research line. Probably, the absence of theoretical understanding of the phenomenon is partially responsible for this.

The theoretical studies of ratchet transport in asymmetric 2DES structures in the form of semidisks Galton board have been started in [26] and further developed in [27,28]. They used extensive numerical simulations of dynamical equations in combination with simple analytical estimates. A rigorous analytical approach, based on the kinetic equation, has been developed in [29] that allowed to solve exactly a case at a low density of asymmetric scatterers of a specific form. Here we combine all these methods that allows us to obtain a global theoretical description of the photogalvanic effect in asymmetric nanostrutures. The development of such global theory allows to make clear predictions for conditions under which the photogalvanic effect can be used for construction of room temperature detectors of high frequency radiation sensitive to polarization.

The paper has the following structure: Section 2 gives a description of various models of asymmetric nanostructures and represents simple analytical computations compared with numerical simulations; Section 3 describes analytical results based on the kinetic equation and also considers a general question of ratchets in dynamical systems with or without time reversibility; the effects of magnetic field on the photogalvanic current are considered in Section 4; discussion of the results and possible application of the effect are given in Section 5.

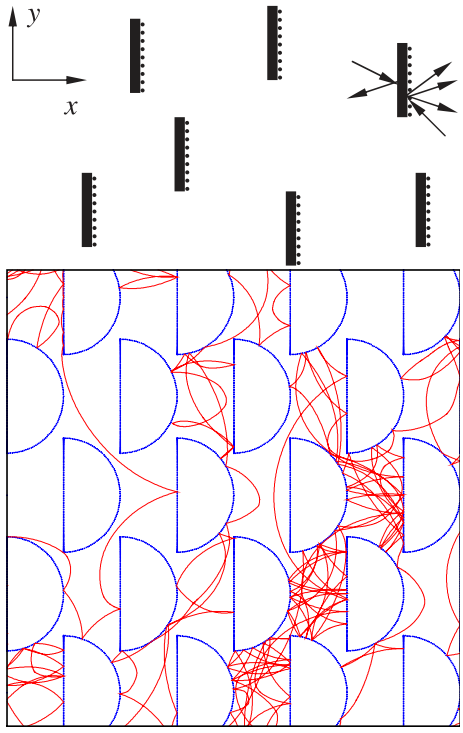


**Fig. 1.** Top panel: the model of oriented scatterers in a form of vertical cuts of length $D$ with a concentration $n_c$. The scattering on cuts is elastic from the left side and diffusive from the right side. The average scattering time on cuts is $\tau_c = 1/(n_c D V_F)$, where $V_F$ is the Fermi velocity of 2DES. Bottom panel: the model of semidisks Galton board, one chaotic trajectory is shown for the system parametes $R/r_d = 2$, $T/E_F = 0.1$, $eEr_d/E_F = 0.3$, $\omega r_d/V_F = 0.67$, $\omega_L/\omega = 2/3$, $\omega\tau_i = \infty$ and $\theta = 0$ (see definition of parameters in Sects. 2 and 4).

## 2 Model description, analytical and numerical results

In our studies we consider two main types of antidots: oriented elastic semidisks and cuts (1D intervals of length $D$) which produce specular reflection from left side and diffusive scattering reflection from right side (see Fig. 1 top panel). The cuts model has been introduced in [29] to mimic effect of scattering on a semidisk (right diffusive side of cut approximately represents circular part of semidisk). The kinetic equation can be solved exactly in this case. For the semidisks Galton board we assume that the semidisks form a triangular lattice (see Fig. 1 bottom panel) with $R$ being a distance between disk centers and $r_d$ being the disk radius. Orientation of a semidisk on $(x, y)$-plane and angles of elastic scattering are shown in Figure 2. For the case of cuts, as in [29], it is assumed that the cuts are irregularly distributed in space with a concentration of cuts in a unit area being $n_c$ (all cuts are vertical as in Fig. 1). The kinetic theory [29] also works in a case of regular lattice of cuts if their density is low.

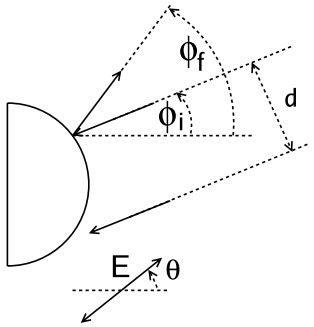


**Fig. 2.** Geometry of the semidisk scatterer in $(x, y)$-plane and definition of the angle notations. A trajectory colliding with the semidisk at an angle $\phi_i$ is scattered at an angle $\phi_f$, which depends on the impact parameter $d$; the electric field $E$ is linear-polarized under angle $\theta$ to $x$-axis.

In the limit of low density of scatterers (cuts or disks) the scattering time $\tau_c$ is

$$\begin{aligned} \tau_c &= 1/(n_c D v) \ \text{(cuts)}, \\ \tau_c &= \sqrt{3}R^2/(8 r_d v) \ \text{(semidisks)}, \end{aligned} \tag{1}$$

where $v$ is the particle velocity (for the Fermi gas $v = V_F$ where $V_F$ is the Fermi velocity of 2DES). In addition to

scattering on antidots we assume that there is also scattering on impurities which is characterized by the scattering time $\tau_i$ (see [28,29]). Between the collisions with antidots and impurities the electron motion is affected only by an electric microwave field $\mathbf{E}\cos\omega t$ linear-polarized under angle $\theta$ to $x$-axis (see Fig. 2). The force acting on electron is $\mathbf{F} = e\mathbf{E}$ and the electron velocity at time $t + \tau_s$ is

$$\mathbf{v}(t+\tau_s) = \mathbf{v}(t) + \frac{2e\mathbf{E}}{m\omega}\cos(\omega t + \omega\tau_s/2)\sin(\omega\tau_s/2), \quad (2)$$

where $e$, $m$ are electron charge and mass.

To find the velocity of stationary flow induced by microwave oscillations we assume that without microwave the equilibrium distribution of electron velocities is given by the Maxwell or the Fermi-Dirac distributions at temperature $T$. Also it is assumed that the microwave field is relatively weak and it only slightly perturbs the equilibrium distribution. Let us start for simplicity from the case of the Maxwell distribution $f_M(\mathbf{v}) = \exp(-m\mathbf{v}^2/2T)/Z$ (here $Z$ is the normalization constant). Then, according to (2), the perturbed distribution is

$$f(\mathbf{v}, t, \tau_s) = f_M(\mathbf{v}) \times \exp\left[\frac{2e\mathbf{v}\mathbf{E}\cos(\omega t + \omega\tau_s/2)\sin(\omega\tau_s/2)}{T\omega}\right], \quad (3)$$

where we omit the velocity independent terms.

To compute the ratchet velocity we first consider the cuts model. We also make certain simplifications which allow to understand the physical origin of the ratchet transport keeping a more rigorous treatment for the next section. Thus, we compute the averaged perturbed distribution function. It is obtained by averaging $f(\mathbf{v}, t, \tau_s)$ over all initial times $t$ and the free flight time $\tau_s$.

$$f_c(\mathbf{v}) = \left\langle \int_0^\infty p_c(\tau) f(\mathbf{v}, t, \tau_s) d\tau_s \right\rangle_t \quad (4)$$

here $p_c(\tau_s)$ is the probability that the scattering occurs after a time $\tau_s$. Its exact expression depends on the geometry of the sample and temperature, but for simplicity we may assume that $p_c(\tau_s) = \exp(-\tau_s/\tau_c)/\tau_c$ where $\tau_c$ is the mean scattering time. Expanding the exponent up to a second order in $\mathbf{E}$ and averaging over $t, \tau_s$ gives:

$$f_c(\mathbf{v}) = f_M(\mathbf{v})\left(1 + \frac{(\tau_c \mathbf{v} e\mathbf{E})^2}{T^2}\frac{1}{1+(\tau_c\omega)^2}\right) \quad (5)$$

with this distribution we can compute the ratchet flow velocity $v_{f,x}$ (in $x$ direction) considering only one scattering on a cut. Indeed, $v_{f,x}$ is the sum of two terms originated from scatterings on the two sides of a cut $v_{f,x} = v_{+,x} - v_{-,x}$. The contribution from the right side is $v_{+,x} = \langle|\mathbf{v}|\rangle/\pi$ since the outgoing direction of the particle is random and the average depends only on the magnitude of the velocity before scattering $|\mathbf{v}|$. On the contrary the scattering on the left side just changes the sign of the velocity in the $x$ direction: $v_x$, as a consequence $v_{-,x} = \langle v_x \eta(v_x)\rangle$ where $\eta(v_x)$ is the step theta-function. The $1/\pi$ factor in the expression of $v_{+,x}$ originates from the averaging over the random scattering angle, it is not present for $v_{-,x}$ since the scattering on the left side of the cut is elastic and no additional averaging is needed. If the distribution is isotropic these two averages are equal, keeping this fact in mind we may compute the contribution to $v_{+,x}, v_{-,x}$ only from the anisotropic (non equilibrium) part of $f_c(\mathbf{v})$. This gives

$$v_{f,x} = v_{+,x} - v_{-,x} = \frac{3\tau_c^2 e^2 E^2}{2\sqrt{2\pi m^3 T}}\frac{1}{1+(\tau_c\omega)^2} \times \left(\frac{1}{\pi}\int_0^{2\pi}\cos^2(\phi-\theta)d\phi - \int_{-\pi/2}^{\pi/2}\cos^2(\phi-\theta)\cos(\phi)d\phi\right) = -\frac{\tau_c^2 e^2 E^2}{2\sqrt{2\pi m^3 T}}\frac{1}{1+(\tau_c\omega)^2}\cos(2\theta), \quad (6)$$

where $\phi$ is the polar angle of the velocity $\mathbf{v}$, $\theta$ is the polarization angle and the coefficient comes from the average value of $\langle v^4\rangle$ computed over the equilibrium distribution $f_M$.

Similar computations give the ratchet velocity $v_{f,y}$ in $y$-direction. Here the contribution from the right cut side vanishes $v_{+,y} = 0$ since after a random scattering the directions with $\phi$ and $-\phi$ have equal probability. The contribution from the left side is given by $v_{-,y} = \langle v_y \eta(v_x)\rangle$:

$$v_{f,y} = v_{-,y} = \frac{3\tau_c^2 e^2 E^2}{2\sqrt{2\pi m^3 T}}\frac{1}{1+(\tau_c\omega)^2} \times \left(\int_{-\pi/2}^{\pi/2}\cos^2(\phi-\theta)\sin(\phi)d\phi\right) = \frac{\tau_c^2 e^2 E^2}{\sqrt{2\pi m^3 T}}\frac{1}{1+(\tau_c\omega)^2}\sin(2\theta). \quad (7)$$

As a result equations (6, 7) give the angle $\psi$ of the direction of ratchet flow ($\tan\psi = v_{f,y}/v_{f,x}$) as a function of polarization angle $\theta$:

$$\tan(\psi) = -2\tan(2\theta). \quad (8)$$

It is important to note that in the computations above we assumed that a scattering event definitely occurs after time $\tau_c$. This model is rather convenient for numerical simulations that allows to make a comparison with the above theoretical estimates. Such a model corresponds to scattering events randomly placed in time. For a static random distribution of cuts in space one should compute the scattering probability with a transport cross section that gives a numerical factor 3 instead of 2 in equation (8) (see next section).

Also above it is assumed that there are no impurities. In their presence the result is proportional to the probability of scattering on antidots which is equal to the ratio $\tau_i/(\tau_i+\tau_c) = \tau/\tau_c$ due to time ergodicity. Here and below $\tau = \tau_c\tau_i/(\tau_c+\tau_i)$ is the relaxation time scale determined by the geometrical mean of $\tau_i$ and $\tau_c$. Hence, in presence of impurities the ratchet velocity is given by

$$\mathbf{v_f} = \frac{\tau^3 e^2 E^2}{2\tau_c\sqrt{2\pi m^3 T}}\frac{1}{1+(\omega\tau)^2}\begin{pmatrix}-\cos(2\theta)\\ 2\sin(2\theta)\end{pmatrix} \quad (9)$$

where up and down terms correspond to $x$ and $y$ components of the ratchet velocity.

The method described above can be also applied to another form of antidots, e.g. for semidisks. The main difference from the cut model is that the direction after collision $\phi_f$ is no longer completely determined by the impact angle $\phi_i$ nor completely random (see Fig. 2). In fact, it is given by a conditional probability $g(\phi_f|\phi_i)$ that depends on the geometry of the scatterer. Due to the scatterer asymmetry, in general, this distribution is not invariant under $y$-axis mirror symmetry. To obtain the expression of $g(\phi_f|\phi_i)$ for a semidisk scatterer it is convenient to represent $g$ via two parts:

$$g(\phi_f|\phi_i) = \begin{cases} g_+(\phi_f|\phi_i), & \phi_i \in (-\pi/2, \pi/2) \\ g_-(\phi_f|\phi_i), & \phi_i \in (\pi/2, 3\pi/2). \end{cases} \quad (10)$$

Let us first compute the contribution to $g$ from collisions with negative $x$ impact velocity $g_+$ that correspond to impact angles $\phi_i \in (-\pi/2, \pi/2)$. The scattering is elastic on all sides of the semidisk. Integrating over the impact parameter $d$ (see Fig. 2) gives the conditional probability $g_+(\phi_f|\phi_i)$ of scattering in the direction $\phi_f$ assuming a collision with an impact angle $\phi_i$,

$$g_+(\phi_f|\phi_i) = \frac{\cos\frac{\phi_f-\phi_i}{2}}{2(1+\cos\phi_i)} \chi_{[\phi_i-\pi,\pi-\phi_i]}(\phi_f) \quad (11)$$

here $\chi_{[\phi_i-\pi,\pi-\phi_i]}$ is the characteristic theta-function of the interval $[\phi_i-\pi, \pi-\phi_i]$. After scattering with an impact angle $\phi_i$ some values of the outgoing angle $\phi_f$ are forbidden since the trajectory can not cross the bulk of the scatterer, for example $\phi_i + \pi$ is always forbidden, the $\chi$ function incorporates this restriction into $g_+(\phi_f|\phi_i)$.

The contribution from the trajectories with positive $x$ impact velocities is given by the distribution $g_-(\phi_f|\phi_i)$ for impact angles in the interval $\phi_i \in (\pi/2, 3\pi/2)$. The resulting conditional probability $g_-(\phi_f|\phi_i)$ splits in two terms: the first comes from the collision with the straight edge of the semidisk and is expressed as a delta function, the second is related to the collisions with the curved edge and is similar to the expression given in equation (11). Hence,

$$g_-(\phi_f|\phi_i) = \frac{2|\cos\phi_i|}{1+|\cos\phi_i|}\delta(\phi_f+\phi_i-2\pi) + \frac{|\cos\frac{\phi_f-\phi_i}{2}|}{2(1+|\cos\phi_i|)}\chi_{[-|\pi-\phi_i|,|\pi-\phi_i|]}(\phi_f). \quad (12)$$

One can check that the distributions obtained in equations (11, 12) are normalized to 1. This normalization corresponds to the conservation of the number of particles after collision: $\int_0^{2\pi} g_+(\phi_f|\phi_i)d\phi_f = \int_0^{2\pi} g_-(\phi_f|\phi_i)d\phi_f = 1$.

Another effect that was not taken into account in the cuts model is that the scattering probability depends on the impact angle $\phi_i$. The probability $g_c(\phi_i)$ that the collision occurs under the angle $\phi_i$ is proportional to the length of the segment obtained by projecting the semidisk on a parallel to the impact direction: $r_d(1+|\cos(\phi_i)|)$, this leads to the probability distribution

$$g_c(\phi_i) = \frac{1+|\cos\phi_i|}{2(2+\pi)}. \quad (13)$$

The distributions given by equations (11–13) and the distribution function $f_c(\mathbf{v})$ (5) give the ratchet velocities via expressions:

$$v_{f,x} = \int_0^{2\pi} d\phi_f \int d^2\mathbf{v}|\mathbf{v}|\cos(\phi_f) g(\phi_f|\phi_i) g_c(\phi_i) f_c(\mathbf{v})$$
$$v_{f,y} = \int_0^{2\pi} d\phi_f \int d^2\mathbf{v}|\mathbf{v}|\sin(\phi_f) g(\phi_f|\phi_i) g_c(\phi_i) f_c(\mathbf{v}). \quad (14)$$

In the calculation of these integrals it turns out that the isotropic (equilibrium) term of $f_c(\mathbf{v})$ vanishes that corresponds to the absence of the effect at equilibrium. In the contribution of the anisotropic term of equation (5) only the angular integrals are different from equations (6, 7) while the integral on $|\mathbf{v}|$ is identical and leads to the same dependence on system parameters. As a result we obtain

$$\mathbf{v_f} = \frac{\pi\tau^3 e^2 E^2}{2(2+\pi)\tau_c\sqrt{2\pi m^3 T}} \frac{1}{1+(\omega\tau)^2} \begin{pmatrix} -\cos(2\theta) \\ \sin(2\theta) \end{pmatrix}. \quad (15)$$

To check the obtained theoretical expressions (9) and (15) we performed numerical simulations of the cuts and semidisks models. The dynamical equations are solved numerically between collisions. The Maxwell equilibrium at temperature $T$ is generated with the help of the Metropolis thermalization algorithm as it is described in [28]. The computation time along one trajectory is about few hundred thousands of microwave periods. The angular dependence of the ratchet velocity is shown in Figures 3, 4. It is in a very good agreement with the obtained theoretical expressions both for the cuts and semidisks models. The fluctuations present in the numerical data are related to the statistical fluctuations in the Maxwell equilibrium. Also sufficiently long trajectories should be used to separate directed ratchet transport compared to diffusive spreading. The statistical error bars are on the level of 10% for the data shown in Figures 3, 4. We will consider the dependence on the parameters $\tau_c, \tau_i$ in the next section.

## 3 The kinetic equation approach

The approach described above can be also used for the Fermi-Dirac equilibrium distribution. However, it if more convenient to use a more general approach based on the kinetic equation which reads:

$$\frac{\partial f}{\partial t} + e\mathbf{E}\cos\omega t \frac{\partial f}{\partial \mathbf{p}} = -\frac{f-f_0}{\tau}, \quad (16)$$

where $f_0$ is an unperturbed equilibrium distribution, $\mathbf{p} = m\mathbf{v}$. The solution can be presented in a form of expansion

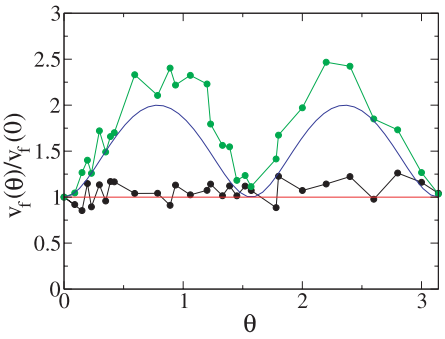


**Fig. 3.** Dependence of the rescaled absolute value of ratchet velocity $v_f(\theta)/v_f(\theta=0)$ on the polarization angle $\theta$ for the cuts and semidisks models (angle is given in radians). For the the semidisk scatterers (black/black curve with circular dots with values close to 1 on the vertical axis) the lattice constant is set to $R/r_d = 4.5$, the impurity scattering time is $\tau_i \approx 15 r_d/v_T$ and the Maxwell equilibrium distribution is characterized by a temperature $T$. With these settings the numerically determined average time interval between two successive collisions with semidisks is $\tau_c \approx 0.77\tau_i \approx 11 r_d/v_T$ (we note that the theoretical scattering time is $\tau_c \approx 4.4 r_d/v_T$ with the thermal velocity $v = v_T = \sqrt{(2T/m)}$ in Eq. (1)). In the simulations for the cuts model (green/gray curve with circular dots and values close to 2.2 on the vertical axis at $\theta = 1.$) the temperature $T$ and the time scales $\tau_c$, $\tau_i$ are taken to be the same as their numerical values in the semidisks case. In both cases the microwave field amplitude and frequency are $eEr_d/T = 0.4$ and $\omega r_d/\sqrt{2mT} = 0.316$. The smooth curves represent the theoretical predictions of equation (9) (blue/black curve for the cuts model) and equation (15) (red/gray straight line for the semidisks model).

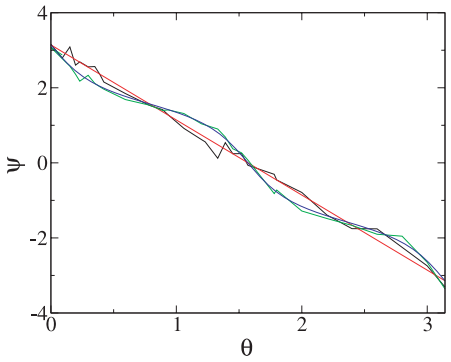


**Fig. 4.** Dependence of the angle $\psi$ of the ratchet flow direction on the polarization angle $\theta$ for the parameters of Figure 2 with the same choice of colors: red/gray straight line for theory ($\psi = \pi - 2\theta$) and black curve fluctuating near it for numerical data in the semidisks model; blue/black smooth curve for theory (see Eq. (8)) and green/gray curve fluctuating near it for numerical data in the cuts model; angles are given in radians.

over powers of external weak field: $f = f_0 + f_1 + f_2 + ...$ The first term is

$$f_1(\mathbf{p},t) = -\frac{\tau e \mathbf{E}\mathbf{v}}{2(1+i\omega\tau)}\frac{\partial f_0}{\partial \epsilon}\exp(i\omega t) + CC, \qquad (17)$$

where $CC$ is a complex conjugated part. The time averaged correction of $f_2$ gives

$$\langle f_2(\mathbf{p},t)\rangle_t = -\tau e\mathbf{E}\langle \cos\omega t \frac{\partial f_1}{\partial \mathbf{p}}\rangle \approx \frac{(\tau e \mathbf{E}\mathbf{v})^2}{2(1+(\omega\tau)^2)}\frac{\partial^2 f_0}{\partial \epsilon^2}, \qquad (18)$$

where we use an approximation that the isotropic term originating from the term $\partial f_1/\partial \mathbf{v}$ does not contribute to the ratchet velocity and therefore can be omitted. Also we assume that the relaxation time $\tau$ is independent of particle energy. The correction (18) has the same form as in equation (5). Thus, for example,

$$v_{f,x} = \langle|v|\rangle/\pi - \langle v_x \eta(v_x)\rangle = -\frac{(em\tau E)^2}{6(1+(\omega\tau)^2)}\cos(2\theta)\int_0^\infty v^4 \frac{\partial^2 f_0(v)}{\partial \epsilon^2} dv$$

and for the Fermi-Dirac distribution at $T \ll E_F$ we obtain the ratchet flow velocity for the cuts model

$$\mathbf{v_f} = \frac{\tau^3 e^2 E^2}{2\pi\tau_c\sqrt{2m^3 E_F}}\frac{1-\pi^2T^2/(24E_F^2)}{1+(\omega\tau)^2}\begin{pmatrix}-\cos(2\theta)\\ 2\sin(2\theta)\end{pmatrix} \qquad (19)$$

while for the semidisks model

$$\mathbf{v_f} = \frac{\pi\tau^3 e^2 E^2}{2(2+\pi)\tau_c\sqrt{2m^3 E_F}}\frac{1-\pi^2T^2/(24E_F^2)}{1+(\omega\tau)^2}\begin{pmatrix}-\cos(2\theta)\\ \sin(2\theta)\end{pmatrix}. \qquad (20)$$

The angle dependence remains the same as for the Maxwell equilibrium.

The case of weak asymmetry can be also treated in a more formal way based of the Green function formalism in the kinetic equation. First we note that in the second order on alternating electric field the components of steady-state current density can be described by phenomenological expressions

$$j_x = \alpha_{xxx}|E_x|^2 + \alpha_{xyy}|E_y|^2,$$
$$j_y = \mathrm{Re}(\alpha_{yxy})(E_x E_y^* + E_x^* E_y) + \mathrm{Im}(\alpha_{yxy})[\mathbf{E}\mathbf{E}^*]_z. \qquad (21)$$

The components of the photogalvanic tensor $\alpha_{xxx}$, $\alpha_{xyy}$ and $\mathrm{Re}(\alpha_{yxy})$ determine the response to the linear-polarized microwave field. For linear polarization along $x$ or $y$ axes the current flows along the $x$ direction; the current in $y$ direction appears for a tilted linear-polarized electric field.

The kinetic equation written in the operator form reads

$$\frac{\partial f}{\partial t} + \hat{F}f = \hat{I}f, \qquad (22)$$

where $f(p,\phi)$ is the distribution function and $\mathbf{p} = p(\cos\phi, \sin\phi)$ is the electron momentum. The term $(\hat{F}f)$ represents the action of electric field $\mathbf{E}(t) = \mathrm{Re}(\mathbf{E}_\omega e^{-i\omega t})$

of the electromagnetic wave with the complex amplitude $\mathbf{E}_\omega = \mathbf{E}^*_{-\omega}$:

$$\hat{F} = e\mathbf{E}(t)\frac{\partial}{\partial \mathbf{p}} = e\left[E_x\left(\cos\phi\frac{\partial}{\partial p} - \frac{\sin\phi}{p}\frac{\partial}{\partial\phi}\right) + E_y\left(\sin\phi\frac{\partial}{\partial p} + \frac{\cos\phi}{p}\frac{\partial}{\partial\phi}\right)\right] \equiv \frac{1}{2}\hat{F}_\omega e^{i\omega t} + CC. \quad (23)$$

The term $\hat{I}f$ is the collision integral

$$\hat{I}f(p,\phi) = \int_0^{2\pi} d\phi'[W(\phi',\phi)f(p,\phi') - W(\phi,\phi')f(p,\phi)], \quad (24)$$

where $W(\phi',\phi)$ is the scattering probability.

The stationary solution of the kinetic equation in the second order of electric field can be written as

$$\overline{f}_2 = \frac{1}{2}\mathrm{Re}\Big(\hat{G}^0\hat{F}_\omega\hat{G}^\omega\hat{F}_{-\omega}f_0\Big) \quad (25)$$

where $\hat{F}_\omega = e\mathbf{E}_\omega\frac{\partial}{\partial\mathbf{p}}$, $\hat{G}$ is the Green function of kinetic equation. For small asymmetry

$$\hat{G}^\omega = \frac{1}{i\omega - 1/\tau} - \frac{1}{(i\omega - 1/\tau)^2}\hat{I}^-, \quad (26)$$

where $\hat{I}^-$ is the antisymmetric part of scattering operator on cuts, semidisks etc. The quantity $\tau = \tau_i\tau_c/(\tau_i+\tau_c)$ can be attributed to the symmetric part of scattering on cuts and to the impurity relaxation time $\tau_i$.

The photogalvanic current reads

$$j_i = \frac{e^3}{4\pi^2}\mathrm{Re}\int d\mathbf{p}\Big\{\tau^2\hat{I}^-\left(\mathbf{E}_{-\omega}\frac{\partial}{\partial\mathbf{p}}\right)\frac{\tau}{1-i\omega\tau}(\mathbf{E}_\omega\mathbf{v})f_0' + \tau\left(\mathbf{E}_{-\omega}\frac{\partial}{\partial\mathbf{p}}\right)\hat{I}^-\frac{\tau^2}{(1-i\omega\tau)^2}(\mathbf{E}_\omega\mathbf{v}f_0')\Big\} \quad (27)$$

here $\mathbf{v} = \mathbf{p}/m$ is the electron velocity, $f_0(\varepsilon)$ is the equilibrium distribution function in energy $\epsilon$, prime means derivative over energy.

From equation (27) we find the current induced by the linear polarized microwave field

$$j_i = \frac{e^3}{4\pi^2}\mathrm{Re}\int d\mathbf{p}\left\{\tau^2 v_i\hat{I}^- v_j v_k\left(\frac{\tau f_0'}{1-i\omega\tau}\right)' - \frac{\tau^2\tau' f_0'}{(1-i\omega\tau)^2}v_i v_j\hat{I}^- v_k\right\}E_jE_k. \quad (28)$$

We use the identities $\hat{I}\xi(\epsilon) = 0$, $\langle\hat{I}\chi(\mathbf{p})\rangle = 0$, and $\langle p_ip_j\hat{I}p_k\rangle = -\langle p_k\hat{I}p_ip_j\rangle$, where $\xi(\epsilon)$ is an arbitrary function of energy, $\chi(\mathbf{p})$ is an arbitrary function of momentum; angular brackets stand for the operation of average over angles in $\mathbf{p}$-space: $\langle ...\rangle = \int\frac{d\phi}{2\pi}(...)$. The first and the second identities follow from the conservation of number of particles, the third is the consequence of the detailed balance principle according to which the probability of transition has the symmetry $W(\mathbf{p}',\mathbf{p}) = W(-\mathbf{p},-\mathbf{p}')$.

Further we consider an algebraic energy dependencies of relaxations times: $\tau,\tau_c \propto \varepsilon^s$. This dependence corresponds to the scattering on a geometric impediment with $\hat{I}^- = (1/\tau_c)\hat{\mathcal{I}}^-$ where the operator $\hat{\mathcal{I}}^-$ is the integral operator on $\phi$, $\tau_c$ is the characteristic time of scattering on cuts or half-disks which depends on the concentration of scatterers $n_c$. The power $s = -1/2$ corresponds to scattering on impurities/scatterers with fixed density in space. We note that $s = 3/2$ may correspond to a case of charged non-screened impurities distributed in the system plane. equation (28) can be transformed to the form:

$$j_i = \frac{e^3m}{2\pi}\int d\varepsilon f_0'\frac{v^3\tau^3}{\tau_c\varepsilon(1+\omega^2\tau^2)}\left\{(2-2s)a_{jki} + \frac{s(1-\omega^2\tau^2)}{(1+\omega^2\tau^2)}a_{ijk}\right\}E_jE_k, \quad (29)$$

where $\mathbf{v} = v\mathbf{u}$, $a_{ijk} = \langle u_iu_j\hat{\mathcal{I}}^-u_k\rangle$ and $\mathbf{u}$ is a unitary vector. The stationary current $j_i = \alpha_{ijk}E_{\omega j}E^*_{\omega k}$ under linear polarized field is given by the following components of photogalvanic tensor (see Figs. 1, 2): $\alpha_{xxx}, \alpha_{xyy}$ and $\mathrm{Re}(\alpha_{yxy})$. At $T = 0$ (a degenerate Fermi gas) the expressions for these components read

$$\alpha_{xxx} = -\frac{e^3V_F\tau^3}{\pi\tau_c(1+\omega^2\tau^2)}\Big[(2-2s) + \frac{s(1-\omega^2\tau^2)}{(1+\omega^2\tau^2)}\Big]a_{xxx}, \quad (30)$$

$$\alpha_{xyy} = \frac{e^3V_F\tau^3}{\pi\tau_c(1+\omega^2\tau^2)} \times\Big[(2-2s)a_{xxx} - \frac{s(1-\omega^2\tau^2)}{(1+\omega^2\tau^2)}a_{xyy}\Big], \quad (31)$$

$$\mathrm{Re}(\alpha_{yxy}) = -\frac{e^3V_F\tau^3}{\pi\tau_c(1+\omega^2\tau^2)}\Big[(2-2s)a_{xyy} + \frac{s(1-\omega^2\tau^2)}{2(1+\omega^2\tau^2)}(a_{xyy}-a_{xxx})\Big]. \quad (32)$$

Here, $\tau,\tau_c$ are relaxation times taken at $\varepsilon = \varepsilon_F$. Now it is necessary to calculate two quantities $a_{xxx}$ and $a_{xyy}$. They depend on the model of asymmetric scatterers. For the case of cuts the scattering probability has the form:

$$W(\phi',\phi) = {\tau_c}^{-1}[\cos\phi'\ \theta(\cos\phi')\delta(\phi'+\phi-\pi) - \frac{1}{2}\cos\phi'\cos\phi\ \theta(\cos\phi)\theta(-\cos\phi')]. \quad (33)$$

Using equation (33) we obtain $a_{xxx} = 1/48$, $a_{xyy} = -1/16$. As a result we have in this model:

$$\alpha_{xxx} = -\frac{e^3V_F\tau^3}{48\pi\tau_c(1+\omega^2\tau^2)^2}[2-s+(2-3s)\omega^2\tau^2], \quad (34)$$

$$\alpha_{xyy} = \frac{e^3V_F\tau^3}{48\pi\tau_c(1+\omega^2\tau^2)^2}[2+s+(2-5s)\omega^2\tau^2], \quad (35)$$

$$\mathrm{Re}(\alpha_{yxy}) = \frac{e^3 V_F \tau^3}{24\pi\tau_c(1+\omega^2\tau^2)^2}[(3-2s)+(3-4s)\omega^2\tau^2)]. \quad (36)$$

The formulas (34, 35, 36) with $s=-1/2$ follow also from the exact solution of the problem for cuts obtained in [29].

According to the previous Section for the semidisks model the scattering probability is

$$W(\phi',\phi) = \frac{1}{\tau_c}\Big\{\cos\phi'\ \theta(\cos\phi')\delta(\phi'+\phi-\pi) + \frac{1}{4}|\sin(\frac{\phi'-\phi}{2})|\big[\theta(\phi-\phi')\theta(-\phi'-\phi) + \theta(\phi'-\phi)\theta(\phi'+\phi)\big]\Big\}. \quad (37)$$

This probability $W$ leads to the following results for the photogalvanic coefficients in the semidisks model:

$$\alpha_{xxx} = -\alpha_{xyy} = -\mathrm{Re}(\alpha_{yxy}) = -\frac{e^3 V_F \tau^3}{12\pi\tau_c(1+\omega^2\tau^2)^2}[2-s+(2-3s)\omega^2\tau^2]. \quad (38)$$

In the numerical simulations for the cuts model it was taken that $\tau$ is independent of energy ($s=0$). In such a case from the above equations (34–36) and equation (38) we obtain

$$\alpha_{xxx} = -\alpha_{xyy} = -\frac{1}{3}\mathrm{Re}(a_{yxy}) = -\frac{e^3\tau^3\sqrt{2}n_e}{24m\sqrt{m\varepsilon_F}\tau_c(1+\omega^2\tau^2)} \quad \text{(cuts)}; \quad (39)$$

$$\alpha_{xxx} = -\alpha_{xyy} = -\mathrm{Re}(a_{yxy}) = -\frac{e^3\tau^3\sqrt{2}n_e}{6\tau_c m\sqrt{m\varepsilon_F}(1+\omega^2\tau^2)} \quad \text{(semidisks)}, \quad (40)$$

where $n_e$ is the electron density related to the current by the relation $\mathbf{j} = en_e\mathbf{V_f}$.

Let us also note that at $\tau$ = const. for the case of Maxwell equilibrium we obtain

$$\alpha_{xxx} = -\alpha_{xyy} = -\frac{1}{3}\mathrm{Re}(a_{yxy}) = -\frac{\sqrt{2\pi}n_e\tau^3 e^3}{24m\sqrt{mT}\tau_c(1+\omega^2\tau^2)} \quad \text{(cuts)}, \quad (41)$$

$$\alpha_{xxx} = -\alpha_{xyy} = -\mathrm{Re}(a_{yxy}) = -\frac{\sqrt{2\pi}n_e\tau^3 e^3}{6m\sqrt{mT}\tau_c(1+\omega^2\tau^2)} \quad \text{(semidisks)}. \quad (42)$$

It is important to note that the relation $\alpha_{xxx} = -\alpha_{xyy}$, which is valid for semidisk antidots at any $s$, implies that the total photogalvanic current is zero for depolarized radiation. For a general form of scatterers and $\tau$ dependent on energy ($s \neq 0$) even depolarized radiation produce nonzero photogalvanic current. This is for example the case for the cuts model with fixed density of impurities where $s=-1/2$.

We should again emphasize the difference between formulas obtained using the kinetic equation approach and simplified way which leads to equations (6, 7). The difference in numerical factors appears due to different methods of averaging: in equations (6, 7) it is assumed that the scattering events are randomly distributed in time, while in the kinetic approach it is assumed that the scattering events are randomly distributed in space. A simple way to obtain equations (39–42) is to consider the mean force applied from the electron gas to an asymmetric scatterer. This force is determined by the momentum production on the scatterer, or, in other words, residue of flows of momenta of incident $\int v_x \mathbf{p} Df(\mathbf{p}) d\mathbf{p}/2\pi^2$ and scattered particles. If the anisotropy is weak, the momentum production can be found substituting the expression for distribution function (18) into the collision integral (24). The flow velocity is determined by equating this force per unit area to the friction of electron system, $-\mathbf{P}/\tau$, where $\mathbf{P} = m\mathbf{v}_f n_e$ is the full mean momentum of electron gas. The result obtained in this way is the same as those obtained from the kinetic approach if the mean free time does not depend on the energy (Eqs. (39–42)).

For a direct comparison with numerical simulations it is convenient to rewrite equations (39, 40) to obtain explicit expressions for the ratchet velocity. For the Fermi-Dirac distribution at $T \ll E_F$ this gives for the cuts model

$$\mathbf{v_f} = \frac{S}{24}\begin{pmatrix} -\cos(2\theta) \\ 3\sin(2\theta)\end{pmatrix} \quad (43)$$

and for the semidisks model

$$\mathbf{v_f} = \frac{S}{6}\begin{pmatrix} -\cos(2\theta) \\ \sin(2\theta)\end{pmatrix}, \quad (44)$$

where

$$S = \frac{e^2\tau^3\sqrt{2}E^2}{m\sqrt{mE_F}\tau_c(1+\omega^2\tau^2)} = V_F\frac{(eE\tau V_F)^2\tau}{2E_F^2\tau_c(1+\omega^2\tau^2)}. \quad (45)$$

To compare the polarization dependence given by equations (43–45) (see also Eqs. (41, 42)) with the numerical results shown in Figures 3, 4 we should take into account that in the numerical simulations of the cuts model the collisions with cuts take place always after time $\tau_c$ (random positions of cuts in time) while the computations above assume fixed distribution of scatterers in space that leads to a factor $3\sin(2\theta)$ in equation (43 instead of $2\sin(2\theta)$ in equations (9, 19). A part of this, the functional dependence on parameters is the same in both computations. A slight difference in a numerical coefficient related to different ways of averaging for cuts randomly distributed in time (Eq. (19)) and in space (Eq. (43)).

The comparison of the theoretical dependence on $\tau$, $\tau_c$ (Eqs. (43, 45)) with the numerical data in the cuts model is shown in Figure 5 at different values of microwave

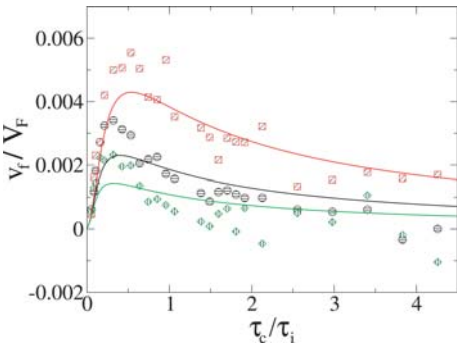


**Fig. 5.** Dependence of the rescaled velocity of ratchet $v_f/V_F$ on the rescaled collision time $\tau_c/\tau_i$ obtained by numerical simulations of the cuts mode (symbols) for $\omega\tau_i = 4.7$; 7.05; 9.4 (red, black, green symbols from top to bottom respectively). The full curves show the theoretical dependence equations (43, 45) for corresponding $\omega\tau_i$ multiplied by a numerical factor $Q = 0.54$. Here, the equilibrium Fermi-Dirac distribution has the temperature $T/E_F = 0.1$ and $eE\tau_i V_F/E_F = 4.2$; the polarization angle $\theta = 0$.

frequency and $\theta = 0$. It shows that the numerical data are well described by the theoretical relation $v_f = -QS/24$ with a numerical factor $Q \approx 0.5$. This confirms that the theory gives a good description of the numerical results.

It is also interesting to compare the theory for the disks model with the numerical data of [28] (see Fig. 8 there). Using the value of $\tau_c$ from equation (1) for a low density at $R/r_d \approx 4$ and $eEr_d/E_F = 0.5$ we obtain from equations (44, 45) $v_f/V_F \approx 0.14$ instead of the numerical value $v_f/V_F \approx 0.05$ (according to Fig. 8 in [28] at $\theta = 0$ and $R/r_d = 4$ we have $\omega\tau \approx 0.8$ since $\tau_i \gg \tau_c$). This means that a numerical factor $Q$ between the theory equations (44, 45) and the numerical simulations [28] is $Q \approx 1/3$. Such a correction can be considered as rather satisfactory since the theory assumes low density approximation which is not yet well justified at $R/r_d = 4$. Also the theory of kinetic equation works in one-collision approximation which may work not so well for completely dynamical systems of semidisks lattice.

Finally, let us return to a simple derivation of the photogalvanic current given in a paragraph after equation (42). According to this consideration the directed flow appears on a time scale of the order of $\tau$. For a purely dynamical system, like the semidisks Galton board, we have $\tau_i = \infty$ and $\tau = \tau_c$. We note that $\tau_c$ is given by equation (1) and is proportional to the inverse Lyapunov exponent of chaotic dynamics in absence of microwave driving. This leads to an interesting *fundamental* question about the photogalvanic current in a purely dynamical system. Indeed, in absence of friction the semidisks Galton board with a monochromatic driving is a Hamiltonian system which has time reversibility property (like $\cos\omega t$), while the appearance of directed current on a time scale $\tau_c$ breaks time reversibility. The dependence of the photogalvanic current on parameters of a real relaxation process is clear from the phenomenological point of view: the current changes its sign with the time inversion while the electric field squared keeps its sign (Eq. (21)). This means that the photogalvanic coefficient $\alpha$ in equation (21) should contain the relaxation constant. By its own, the kinetic equation is irreversible even if only the static potential scatterers are taken into account. In fact, a purely dynamical system is reversible and hence the stationary current should vanish for it. In principle this point can be explained by the dynamical chaos where the time reversibility is broken in practice for a coarse-grained distribution. However, a more delicate point is the question about the detailed balance principle. In a dynamical system it means that the transition probabilities are proportional to a measure in the Hamiltonian phase space and if all phase space is chaotic there should be no global directed current on large time scales. In a sense the numerical results [26] are in favor of this statement since there a small friction force $\mathbf{F_f} = -\gamma\mathbf{p}$ gives the velocity of stationary flow $v_f \sim \gamma R$ which disappears in the limit of $\gamma \to 0$. However, in the limit of small $\gamma$ the situation is somewhat specific since the average steady state energy $E_s$, analogous to temperature, grows with a decrease of $\gamma$ as $E_s \sim ((eE)^2/\gamma)^{2/3} \sim T$ that leads finally to the relations similar to those given by equations (9, 15, 41, 42). The numerical simulations performed in [27] have been done with the Nosè-Hoover dynamics (see [30]) which can be viewed as a purely dynamical time reversible Hamiltonian system in an extended phase space with additional variables. Thus the photogalvanic current can appear in a Hamiltonian asymmetric system with monochromatic driving. However, the directed flow we discussed takes place only in some part of total phase space corresponding to physical variables and it is possible that the total current in total extended phase space still remains zero. Indeed, in principle it is known that in chaotic Hamiltonian systems there may be two separate components (e.g. one with a regular motion and another with a chaotic motion) with a directed current in each component but with the total current equal to zero (see examples in [31]). The ratchet analyzed in [27] with the Nosè-Hoover dynamics can be such a case. Also, the contradiction can be resolved if to assume an existence of a certain time scale after which the photogalvanic current is stabilized. Thus, from a practical view point we may say that in a dynamical chaotic Hamiltonian system signatures of directed flow appear after the time scale $\tau_c$ but since the current velocity $v_f$ it proportional to a second power of weak field $v_f \propto (eE)^2$ a relatively long time $t_r \propto 1/(eE)^2$ is needed to observe this current in presence of chaotic fluctuations and it is necessary that the steady state distribution in energy is established on a time scale which is shorter than $t_r$. Further studies are required to understand more deeply the problem of time reversibility in the context of the photogalvanic effect.

## 4 Effects of a magnetic field for the semidisks Galton board

For experiments on photogalvanic current in asymmetric nanostructures it is important to know what are the effects

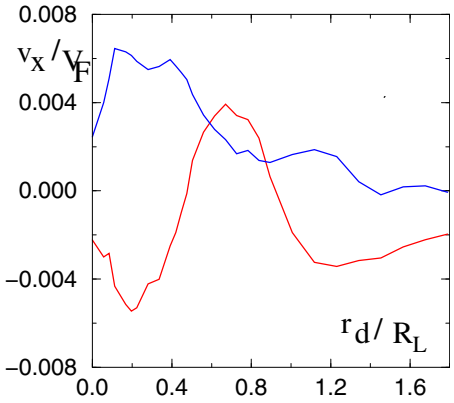


**Fig. 6.** Dependence of rescaled ratchet velocity $v_x/V_F$ in $x$-direction on the ratio $r_d/R_L$ proportional to the magnetic field $B$ perpendicular to the semidisks Galton board. The system parameters are $R/r_d = 2.5$, $T/E_F = 0.1$, $eEr_d/E_F = 0.3$, $l_\omega/r_d = 2\pi V_F/(\omega r_d) = 9$. The bottom (top) red (blue) curve corresponds to the polarization angle $\theta = 0$ ($\theta = \pi/2$). The rescaled mean free path due to impurity scattering is $l/r_d = V_F\tau_i/r_d = 45$; the rescaled computation time is $\omega t = 3.1 \times 10^6$.

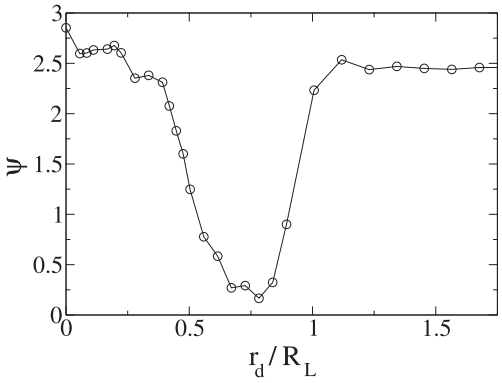


**Fig. 7.** Dependence of ratchet current angle $\psi$ on a rescaled magnetic field $r_d/R_L \propto B$ for the case of Figure 6 at $\theta = 0$; curve with circles shows numerical data, angle is given in radians.

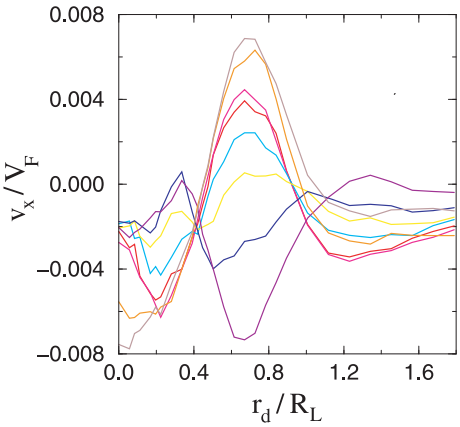


**Fig. 8.** Dependence of the ratchet rescaled velocity $v_x/V_F$ on the rescaled ratio $r_d/R_L \propto B$ for parameters of Figure 6 at $\theta = 0$ and various values of rescaled microwave frequency $\omega r_d/V_F = 0.335$ (brown), 0.447 (orange), 0.648 (magenta), 0.693 (red), 0.805 (cyzen), 0.939 (yellow), 1.12 (blue), 1.39 (violet) (curves from top to bottom at $r_d/R_L = 0.8$).

of a magnetic field $B$ perpendicular to the 2DES plane on the strength of current and its directionality. An analytic solution of the kinetic equation becomes much more complicated compared to the cases considered above. This is especially the case when the Larmor radius $R_L$ of electron motion becomes comparable with the size of asymmetric antidots. Therefore, the numerical simulations in this case become especially important. For the semidisks Galton board the effects of magnetic field have been studied in [28]. They clearly show that the ratchet current becomes quite weak when the Larmor radius $R_L$ becomes smaller then the semidisk radius $r_d$. This is rather natural from a physical view point since in this regime the scattering on semidiscs is suppressed.

However, in the regime with $r_d/R_L \sim 1$ a relatively weak magnetic field can significantly affect the directionality of photogalvanic current. This is illustrated in Figures 6, 7 obtained by numerical simulations with the method described in [28]. The results of these Figures clearly show that a moderate magnetic field can change the direction of current almost on 180 degrees (Fig. 7). The angular dependence of Figure 7 is not sensitive to the microwave field strength and therefore is not related to the Lorentz force. We attribute the origin of this strong angular dependence to a significant change of scattering process in the regime when $r_d/R_L \sim 1$ related to multiple collisions of electron with a semidisk.

To make a more close link to possible experimental studies we note that for the electron density $n_e = 2.5 \times 10^{11}$ cm$^{-2}$, an effective electron mass $m = 0.067m_e$ and the semidisk radius $r_d = 0.4\mu$m we have for the parameters of Figure 6 the following physical values: $E_F \approx 100$ K, $V_F = 2.2 \times 10^7$ cm/s, $\omega/2\pi = 60$ GHz, $l_\omega = 2\pi V_F/\omega = 3.6$ $\mu$m and $l = V_F\tau_i = 18$ $\mu$m (such value of $l$ corresponds to mobility of about $2 \times 10^6$ cm$^2$/V S), a magnetic field $B = 0.075$ T corresponds to the Larmor frequency $\omega_L \approx 34$ GHz and $r_d/R_L = 0.4$. For these parameters and data of Figure 8 the microwave frequency changes from 29 GHz to 120 GHz when the rescaled ratio changes from $\omega r_d/V_F = 0.335$ to 1.39 ($\omega r_d/V_F = 0.693$ for Fig. 6).

In absence of magnetic field there is no dependence of current direction on the microwave frequency. On the contrary, in the regime $r_d/R_L \sim 1$ the directionality of flow can be also changed by changing $\omega$ as it is shown in Figure 8. We also note that the velocity of flow in $x$ direction remains the same with a change $B \to -B$ due to symmetry reasons and we present data only for $B > 0$.

This angular dependence becomes weaker when the mean free path $l$ decreases due to decrease of impurity scattering time $\tau_i$ (see Fig. 9). The results of Fig. 9 also show that the ratchet effect disappears when $l$ becomes smaller than size of asymmetric antidot. Of course, the current is absent when the semidisks are replaced by disks (in this case the numerical data, shown by dashed curve in Fig. 9, are on a level of statistical fluctuations).

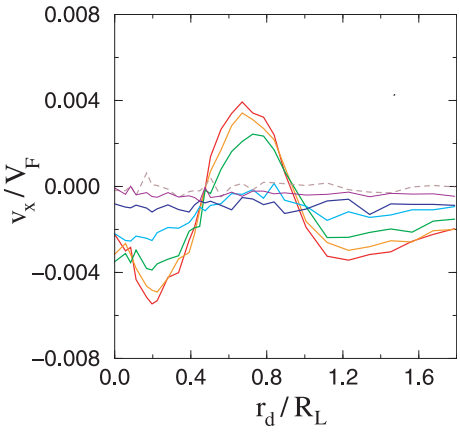


**Fig. 9.** Dependence of the ratchet rescaled velocity $v_x/V_F$ on the rescaled ratio $r_d/R_L \propto B$ for parameters of Figure 6 at $\theta = 0$ and various values of rescaled mean free path $l/r_d = V_F\tau_i/r_d = 45,\ 22.5,\ 11.1,\ 4.5,\ 2.25,\ 1.1$ (full curves from top to bottom at $r_d/R_L = 0.8$; for the physical parameters given in the text $l$ changes from 18 $\mu$m to 0.45 $\mu m$); dashed curve corresponds to the case when semidisks are replaced by disks and $l/r_d = 45$.

The angular dependence of the photogalvanic current $B$ and $\omega$ found in this section is rather nontrivial and further studies are required to obtain a detailed explanation for it.

## 5 Discussion

In this paper we developed a theory which determines the strength and directionality of the phogalvanic current in artificial asymmetric nanostructures. The theoretical results are in good agreement with detailed numerical simulations performed in this work and in [28]. We also find from numerical simulations that the directionality of photogalvanic current is very sensitive to weak magnetic fields.

A microwave field of $E = 1$ V/cm generates in a lattice of semidisks with $R \sim 1$ $\mu$m a current of about 0.2 nA per lattice row at electron density $n_e \approx 2.5\times10^{11}$. For a structure of 100 $\mu$m we have currents of about 20 nA. The photogalvanic effect has classical grounds and exists at room temperature if the mean free path remains larger (or comparable) than the size of asymmetric antidot. This is the case of the Lund experiment [25] with $l \sim R \sim 100$ nm (the polarization there corresponds to $\theta = \pi/2$, triangles are used instead of disks). For a fixed ratio $R/r_d$ a decrease of $R \sim l$ by a factor 10 gives a drop of current by a factor 100, however, the induced voltage drops only by a factor 10 since a resistance also drops 10 times. While the experiments [23,25] demonstrate the existence of the effect there are still no experimental data to be compared with our theoretical and numerical results: in the experiments the strength of current is known but a microwave field strength acting on electrons is not well defined. Also till now only two polarization cases have been analyzed experimentally ($\theta = 0$ in [23] and $\theta = \pi/2$ in [25]). The directionality of current in these experiments is in agreement with our results but a detailed experimental investigation of the polarization dependence is still highly desirable.

All these considerations clearly show that further experimental studies of photogalvanic currents in asymmetric nanostructures are very interesting and important. Indeed, the theory developed above considers only the case of noninteracting particles. In reality electron-electron interaction may play an important role, as well as plasmon modes can also affect the photogalvanic effect. Also at small scales with $R \sim 100$ nm the level spacing between quantum levels inside one lattice cell becomes of the order of 100 GHz (at $n_e \sim 3\times10^{11}$) and quantum effects may play an important role. Also at $R < 100$ nm the collision frequency enters in teraherz range $V_F/R > 1$ THz. Thus such asymmetric nanostructures can be used as room temperature detectors of radiation in teraherz range. In analogy with the GORE-TEX material used in common life for one-way transport of water and air [32] such artificial asymmetric nanostructures may be considered as "NANO-GORE-TEX" material. The further studies of the NANO-GORE-TEX properties may bring new interesting applications including high frequency detectors and sensors.

We thank Z.D. Kvon for useful discussions. This work was supported in part by the ANR PNANO project MICONANO and (for MVE and LIM) by the grant of RFBR No. 04-02-16398, Program for support of scientific schools of the Russian Federation No. 4500.2006 and INTAS No. 03-51-6453. One of us (D.L.S.) thanks the Lewiner Institute for Theoretical Physics at Technion for hospitality at the final stage of this work.

## References

1. A.M. Glass, D. Linde, T.J. Negran, Appl. Phys. Lett. **25**, 233 (1974)
2. I.B. Barkan, M.V. Entin, S.I. Marennikov, Phys. Stat. Sol. A **38**, K139 (1978)
3. V.I. Belinicher, I.F. Kanaev, V.K. Malinovskii, B.I. Sturman, Avtometria **4**, 23 (1976) (in Russian)
4. E. M. Baskin, L. I. Magarill, M. V. Entin, Sov. Phys.-Solid State **20**, 1403 (1978) [Fiz. Tver. Tela **20**, 2432 (1978)]
5. V.I. Belinicher, B.I. Sturman, Sov. Phys. Usp. **23**, 199 (1980) [Usp. Fiz. Nauk **130**, 415 (1980)]
6. F. Jülicher, A. Ajdari, J. Prost, Rev. Mod. Phys. **69**, 1269 (1997)
7. R.P. Feynman, R.B. Leighton, M. Sands, *The Feynman lectures on physics* (Addison Wesley, Reading MA, 1963), Vol. 1, Chap. 46
8. R.D. Astumian, P. Hänggi, Physics Today **55**, 33 (2002)
9. P. Reimann, Phys. Rep. **361**, 57 (2002)
10. J.B. Majer, J. Peguiron, M. Grifoni, M. Tusveld, J.E. Mooij, Phys. Rev. Lett. **90**, 056802 (2003)
11. J.E. Villegas, S. Savel'ev, F. Nori, E.M. Gonzalez, J.V. Anguita, R. Garcia, J.L. Vicent, Science **302**, 1188 (2003)
12. A.V. Ustinov, C. Coqui, A. Kemp, Y. Zolotaryuk, M. Salerno, Phys. Rev. Lett. **93**, 087001 (2004)

13. C. Mennerat-Robilliard, D. Lucas, S. Guibal, J. Tabosa, C. Jurczak, J.-Y. Courtois, G. Grynberg, Phys. Rev. Lett. **82**, 851 (1999)
14. S. Matthias, F. Müller, Nature **424**, 53 (2003)
15. V. Studer, A. Pepin, Y. Chen, A. Ajdari, Analyst **129**, 944 (2004)
16. D. Weiss, M. L. Roukes, A. Menschig, P. Grambow, K. von Klitzing, G. Weimann, Phys. Rev. Lett. **66**, 2790 (1991)
17. G.M. Gusev, Z.D. Kvon, V.M. Kudryashov, L.V. Litvin, Y.V. Nastaushev, V.T. Dolgopolov, A.A. Shashkin, JETP Lett. **54**, 364 (1991) [Pis'ma Zh. Eksp. Teor. Fiz. **54**, 369 (1991)]
18. F. Galton, *Natural inherritance* (Macmillan, London, 1889)
19. I.P. Kornfeld, S.V. Fomin, Ya.G. Sinai, *Ergodic theory* (Springer, Berlin, 1982)
20. R. Fleischmann, T. Geisel, R. Ketzmerick, Phys. Rev. Lett. **68**, 1367 (1992); Europhys. Lett. **25**, 219 (1994)
21. A.A. Bykov, G.M. Gusev, Z.D. Kvon, V.M. Kudryashev, V.G. Plyukhin, Pis'ma Zh. Eksp. Teor. Fiz. **53**, 407 (1991) [JETP Lett. **53**, 427 (1991)]
22. E. Vasiliadu, R. Fleischmann, D. Weiss, D. Heitmann, K.V. Klitzing, T. Geisel, R. Bergmann, H. Schweizer, C.T. Foxon, Phys. Rev. B **52**, R5658 (1995)
23. A. Lorke, S. Wimmer, B. Jager, J.P. Kotthaus, W. Wegscheider, M. Bichler, Phys. B **249–251**, 312 (1998)
24. H. Linke, T.E. Humphrey, A. Löfgren, A.O. Sushkov, R. Newbury, R.P. Taylor, P. Omling, Science **286**, 2314 (1999)
25. A.M. Song, P. Omling, L. Samuelson, W. Seifert, I. Shorubalko, H. Zirath, Appl. Phys. Lett. **79**, 1357 (2001)
26. A.D. Chepelianskii, D.L. Shepelyansky, Phys. Rev. B **71**, 052508 (2005)
27. G. Cristadoro, D.L. Shepelyansky, Phys. Rev. E **71**, 036111 (2005)
28. A.D. Chepelianskii, Eur. Phys. J. B **52**, 389 (2006)
29. M.V. Entin, L.I. Magarill, Phys. Rev. B **72**, 205206 (2006)
30. W. G. Hoover, *Time reversibility, computer simulation, and chaos* (World Scientific, Singapore, 1999)
31. H. Schanz, M.-F. Otto, R. Ketzmerick, T. Dittrich, Phys. Rev. Lett. **87**, 070601 (2001)
32. See e.g., `http://www.gore-tex.com/`